Published in final edited form as:
Journal of the Mechanical Behavior of Biomedical Materials, 2018, 84, 46-53, doi:10.1016/j.jmbbm.2018.04.025

Attachment and spatial organisation of human mesenchymal stem cells on poly(ethylene glycol) hydrogels.

Aman S. Chahal, Manuel Schweikle, Catherine A. Heyward and Hanna Tiainen

Department of Biomaterials, Institute of Clinical Dentistry, University of Oslo, Norway

Corresponding author e-mail: hanna.tiainen@odont.uio.no

Keywords: cell attachment, RGD, PEG, hydrogel, human mesenchymal stem cells, tissue engineering

---

Abstract

Strategies that enable hydrogel substrates to support cell attachment typically incorporate either entire extracellular matrix proteins or synthetic peptide fragments such as the RGD (arginine–glycine–aspartic acid) motif. Previous studies have carefully analysed how material characteristics can affect single cell morphologies. However, the influence of substrate stiffness and ligand presentation on the spatial organisation of human mesenchymal stem cells (hMSCs) have not yet been examined. In this study, we assessed how hMSCs organise themselves on soft (E = 7.4 – 11.2 kPa) and stiff (E = 27.3 – 36.8 kPa) poly(ethylene glycol) (PEG) hydrogels with varying concentrations of RGD (0.05 – 2.5 mM). Our results indicate that hMSCs seeded on soft hydrogels clustered with reduced cell attachment and spreading area, irrespective of RGD concentration and isoform. On stiff hydrogels, in contrast, cells spread with high spatial coverage for RGD concentrations of 0.5 mM or higher. In conclusion, we identified that an interplay of hydrogel stiffness and the availability of cell attachment motifs are important factors in regulating hMSC organisation on PEG hydrogels. Understanding how cells initially interact and colonize the surface of this material is a fundamental prerequisite for the design of controlled platforms for tissue engineering and mechanobiology studies.

1. Introduction

The mechanical properties of biomaterial substrates are known to alter cellular behaviour in many ways (Fusco et al., 2015). Changes in substrate stiffness are capable of altering cellular morphologies as well as guiding cells towards a specific fate (Chicurel et al., 1998; El-Sherbiny and Yacoub, 2013; Engler et al., 2006). This has revolutionised researchers' approaches towards tailoring substrates that communicate with and instruct cells in a manner that supports the application of the biomaterial itself (Li et al., 2017). In addition to the mechanical properties, the presence of anchored biochemical ligands within the substrate can have a significant impact on various cellular behaviours (Bae et al., 2007; Engler et al., 2004; Hsiong et al., 2008; Kilian and Mrksich, 2012; Wen et al., 2014). Cellular structure, motility and proliferation rates can be influenced by altering substrate stiffness or the availability of biochemical ligands (Frith et al., 2012; Mathieu and Loboa, 2012). Poly(ethylene glycol) (PEG) hydrogels are excellent platforms for mechanobiology studies by providing robust and highly controllable systems, allowing for regulated ligand tethering while permitting stiffness tunability (Herrick et al., 2013).

While elaborate studies have investigated changes in single cell morphologies linked to alterations in nanotopography, mechanics and functionality of various substrates, the way in which cells organise in groups or colonies on these substrates has not yet been investigated (Engler et al., 2004; Kim et al., 2012; Schwarz and Bischofs, 2005; Yim et al., 2010). Various studies have controlled the presentation of synthetic cell attachment ligands on patterned surfaces, providing insight into mechanosensing and mechanotransductive processes (Arnold et al., 2004; Deeg et al., 2011; Frith et al., 2012). Studies that have successfully incorporated various concentrations of RGD peptides within hydrogels often encapsulate cells within the gel and test for fate-priming without analysing how cells organise themselves as groups upon initial contact (Anderson et al., 2011; Kyburz and Anseth, 2013; Nuttelman et al., 2004). However, the encapsulation of autologous cells typically requires isolation and expansion, substantially limiting its potential translation to the clinic. Cell-free systems relying on recruitment and attachment of cells from adjacent tissues to the substrate promise a more feasible solution regarding clinical application. To maximise the potential of such approaches, it is crucial that we define a minimum concentration of RGD required in order to accommodate cell attachment.

The low protein adsorption of PEG is advantageous when engineering controlled cell-responsive systems, but requires tethering of sufficient levels of cell attachment motifs in order for the substrate to support cellular adhesion (Hern and Hubbell, 1998). The incorporation of RGD peptides in hydrogel systems have shown to enhance cellular attachment, spreading and proliferation (Shu et al., 2004). Both linear and cyclic isoforms of synthetic RGD peptides have been used in the past (Hersel et al., 2003; Verrier et al., 2002). It is known that the cyclic isoform is selective in binding to the $\alpha_v\beta_3$ integrin subunit, while the linear form is specific to the $\alpha_5\beta_1$ subunit, resulting in the onset of different downstream cascades within the cell (Hersel et al., 2003). Studies related to tissue engineering and stem cell-based regenerative medicine often use cyclic isoforms to guide differentiation processes, since the cyclic isoform is also known to have high stability *in vivo* (Haubner et al., 1996; Hersel et al., 2003; Kantlehner et al., 2000; Zhang et al., 2016). Additional evidence suggests that $\alpha_v\beta_3$ integrin exhibits significantly higher binding affinity and specificity to the cyclic isoform than the linear one (Haubner et al., 1996; Rodda et al., 2014). This proposes that lower concentrations of the cyclic isoform may be required in hydrogels for efficient cell adhesion and survival, compared to the linear isoform, which could in turn also have an impact on the stiffness of the substrate. As indicated by Bellis, many confounding factors make the selection of RGD peptide concentrations and isoforms a complex decision when designing hydrogels (Bellis, 2011).

In this study, we use a hydrogel system based on PEG star macromeres. Maleimide groups at the chain ends serve as functional groups for end-linking of the macromeres into hydrogels as well as ligation sites for tethering RGD peptides. Since the same functional groups are used for tethering RGD peptides as for cross-linking of the hydrogel backbone, one can expect a correlation of RGD peptide concentration and gel stiffness as less elastically active links might be formed when fewer unreacted functional groups are available. We investigate potential changes in substrate stiffness due to increased RGD tethering within this system via nanoindentation, using atomic force microscopy (AFM). We hypothesize that higher RGD concentrations and stiffer gels promote human mesenchymal stem cell (hMSC) attachment and spreading. Hence, we study how hMSCs attach and organise themselves on PEG hydrogels functionalised with varying concentrations of linear or cyclic RGD peptides (linRGD and cycRGD respectively) while implementing image analysis tools to assess organisational changes of cells as initial indicators of how they interact with PEG hydrogels.

2. Methods

2.1 Hydrogel preparation

Hydrogels of distinct stiffness were made from maleimide functionalised PEG star macromeres (PEG-MAL) varying in molecular weight and functionality. All polymers were purchased from JenKem Technology USA. Four-armed PEG-MAL (20 kDa) was dissolved in citrate phosphate buffer with a final buffer concentration of 100 mM within the polymer mix (pH 3), whereas 4-armed PEG-MAL (10 kDa) and 8-arm PEG-MAL (20 kDa) were dissolved in citrate phosphate buffer at pH 2.5. Prior to gel formation, macromeres were either functionalized with Cyclo(RGD(dF)C) produced by AnaSpec or linear RGD peptide (Ac-GCGYGRGDSPG-NH_2) produced by Pepmic, at final concentrations of 0.05, 0.5, 1.5 or 2.5 mM. Four-arm (20 kDa) and 8-arm (20 kDa) gels without any RGD peptides were prepared as controls. A linking peptide (Ac-GCRDVPMSMRGGDRCG-NH2) synthesized by Pepmic was used to end-link the macromeres into gels. In brief, 20 µL of RGD-functionalised PEG-MAL-end-linker mixtures were pipetted between two hydrophobic glass slides separated by a 1 mm spacer and allowed to react at 37°C for 20 min. All gels were swollen for 1 h in 1 mL of mesenchymal stem cell growth media (MSCGM, Lonza) at 37°C in 24-well plates. After swelling, excess medium was discarded in preparation for cell seeding. Three gels were prepared for each RGD concentration, in preparation for cell seeding. Four-arm PEG-MAL (20 kDa) hydrogels are referred to as ‘soft’ hydrogels, whereas 8-arm PEG-MAL (20 kDa) hydrogels are referred to as ‘stiff’ hydrogels in the results and discussion of this paper.

2.2 Swelling ratio measurements

The swelling ratio was defined as the ratio of swollen (V_s) to non-swollen (V_r) volume. Volumes were determined using an analytical scale equipped with a buoyancy kit. Hydrogels were weighed first in air and then in phosphate buffered saline (PBS) immediately after curing. Swollen gels were weighed again at 1.5 h and 48 h after swelling in PBS. Triplicates were prepared for each group and experiments were conducted twice independently (n=6). All measurements were performed at room temperature.

2.3 AFM nanoindentation

Gel stiffness was determined on micro-scale via nanoindentation using a JPK Nanowizard 4 atomic force microscope (AFM). Indentation was performed with colloidal probes with 2 µm SiO_2 spheres attached to tip-less silicon nitride cantilevers (PNP-TR-TL, NanoWorld AG), which were purchased from sQube. Each cantilever was calibrated in a two-step procedure in PBS. First, the optical lever sensitivity was defined by deflecting the cantilever against a hard glass surface, then, the cantilever spring constant was determined using the thermal noise method. Spring constants were typically found around 0.06 N/m.

For nanoindentation experiments, hydrogel disks were prepared as described above and swollen to equilibrium in PBS at 37°C. The disks were placed on glass slides and covered with a PBS droplet. Three force maps of 8 x 8 indentations on an area of 50 x 50 μm^2 were recorded on random spots. A minimum of three gels from independent experiments were tested per group. Maximal indentation force was controlled to 2 nN. E-modulus was determined from the force-indentation curves using the Hertz model. All samples were assumed to behave like ideal gels (Poisson's ratio of 0.5).

2.4 Cell culture and seeding

Experiments were performed using hMSCs purchased from Lonza (lot #0000451491, tissue acquisition #28386). Cells were cultured (passage ≤ 5) at 37°C in a 5% CO_2 incubator in Lonza's Poetics Mesenchymal Stem Cell Basal Medium (catalog no. PT-3238) supplemented with Poetics MSCGM™ hMSC SingleQuot Kit (catalog no. PT-4105) to maintain cells in an undifferentiated state. Once cells were 70% confluent, they were trypsinized for seeding onto glass coverslips and onto hydrogels. A seeding density of 4,700 cells/cm^2 of hydrogel surface area (3,000 per gel in a 30 µL droplet) was used. The surface area covered by the droplets was assessed using contact angle measurements to ensure uniform initial cell seeding density across the gel and glass surfaces. Cells were allowed to attach for 1.5 h before 1 mL of MSCGM was added to each well. hMSCs were cultured on hydrogels and glass substrates for 48 h prior to fixation. Two independent experiments were conducted, each containing triplicates and data for triplicates from each group was pooled.

2.5 Immunolabeling and confocal microscopy

hMSCs were fixed by first adding a 4% paraformaldehyde (PFA) solution directly to the medium (1:1 ratio) for 10 min, before all liquid was discarded. Subsequently, 4% PFA was added to the wells for 20 min. The PFA was discarded and cells were washed with Dulbecco's Phosphate-buffered saline (DPBS) three times. hMSCs were then permeabilized using 0.1% Triton X-100 for 10 minutes, followed by a DPBS rinse. All samples were blocked with 5% bovine serum albumin (BSA) in DPBS blocking buffer for 2 h at room temperature. Blocking buffer was discarded and cells were rinsed three times with DPBS. Mouse anti-human vinculin primary antibody (ABfinity, Thermo Fischer) was diluted 1:100 in 1% DPBS-BSA solution. Cells were incubated overnight at 4°C with primary antibodies. The primary antibodies were discarded, followed by three DPBS rinses, before the secondary antibodies and phalloidin were added to the wells. Phalloidin and all secondary antibodies (Thermo Fischer Scientific) were diluted in 1% BSA-DPBS solution to obtain working dilutions of 1:400. Alexa Fluor® 647 Phalloidin was used for fluorescent labelling of actin and cytoskeleton. Goat anti-mouse IgG secondary antibody Alexa Fluor® 488 was used to fluorescently label anti-vinculin primary antibodies. DAPI was used at a 1:1000 working dilution to stain the nuclei. Gels and glass cover slips were viewed with a 20x/0.40 HCX PL APO CS objective lens on a Leica SP8 confocal microscope using 638 nm excitation and 643-710 nm emission filters for phalloidin and with 488 nm excitation and 493-560 nm emission filters for vinculin. Two additional images were taken per replicate with the same lens and an additional 2x electronic zoom to obtain images for focal adhesion analysis. Z-stacks were generated where cells in the same field of view did not appear on the same plane due to sample topography.

2.6 Data extraction and image analysis

For all data obtained via confocal imaging, 60 fields of view (F.O.V) were analysed per gel group (n=60). However, these 60 F.O.Vs were obtained from two independent experiments, each consisting of triplicates, from which 10 images were taken per replicate. Maximal intensity projections were generated for regions of interest that were imaged as z-stacks. Confocal microscopy images were imported into FIJI Software (ImageJ, NIH) for automated cell area analysis using a custom macro. Briefly,

the macro consisted of removal of outlier pixels, median blur and rolling ball background subtraction, followed by merging of the nuclear and vinculin channels to generate images for whole cell area measurements. Otsu intensity thresholding produced a binary image to allow counting and measuring of all objects above a defined size threshold. Data was expressed as the mean proportion of field of view area covered by cells. Separately, the DAPI channel images were imported into Cell Profiler 2.2.0 for nuclei counting and nearest neighbour analysis. The pipeline comprised of image smoothening with a median blur, background subtraction and rescaling of the image intensities, followed by automatic Otsu thresholding to identify the nuclei and allow assessment of the nearest neighbour distance. We employed a nearest neighbour analysis methodology from Eidet et al. (Eidet et al., 2014) to analyse the spatial arrangement of cells in relation to their neighbours. This was first described by Clark and Evans to measure spatial relationships in populations (Clark and Evans, 1954). This enabled the assessment of the cell distribution within each field of view with the parameter R, which can vary from 0 (clustered) to 2.15 (hexagonal distribution), with R = 1 indicating a random distribution. A sample of this methodology is provided in the supplementary information of this manuscript (Fig. S1).

2.7 Statistical analysis

Statistical analysis was conducted using the software Sigma Plot 13.0 (Systat Software Inc.) One-way ANOVA was performed along with the Dunn's method on all data sets to test for statistical significance. The only exception to this was for swelling ratio data, where t-tests were performed to determine significant differences. Statistic tests were performed where differences between groups show $p < 0.05$. Significant statistical differences are represented in figures by a single asterisk symbol. The spread of data points for all box plots are represented by a central solid line (median), box limits (25^{th} and 75^{th} percentiles) and whiskers denoting upper (90^{th}) and lower (10^{th}) percentiles.

3. Results

3.1 Mechanical properties of the hydrogel substrates

Stiffness of 4-arm (20 kDa) and 8-arm (20 kDa) PEG hydrogels as measured by AFM nanoindentation is shown in Fig. 1. As a control, we also performed nanoindentation on gels without RGD functionalisation (NF gels) as well as 4-arm gels of lower molecular weight (10 kDa). A prominent difference in stiffness can be observed between 4-arm and 8-arm gels. 4-arm "soft" hydrogels show *E* moduli ranging from 7.4 to 11.2 kPa, whereas 8-arm "stiff" hydrogels feature *E* moduli ranging from 27.3 to 36.8 kPa. However, we observe no statistically significant differences in stiffness between gels with varying RGD concentrations for neither the 4-arm nor the 8-arm gels. A noticeably wide spread of data points is seen for all gels, indicative of variations in stiffness of gel batches produced from different reaction mixtures.

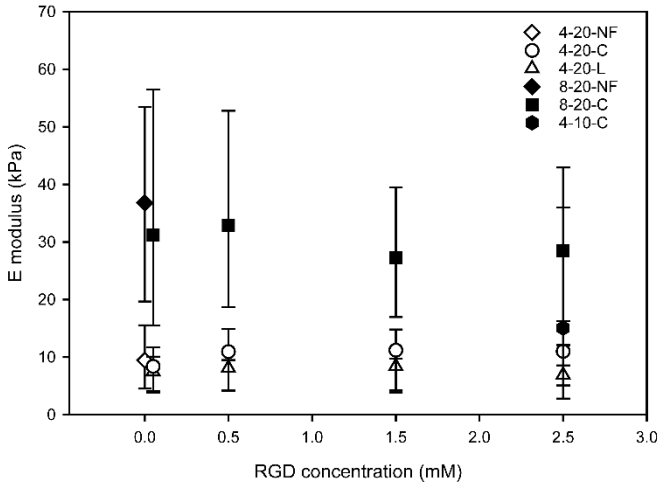

Fig. 1: Differences in stiffness between 4-arm (20 kDa), 8-arm (20 kDa) and 4-arm (10 kDa) hydrogels ($n \geq 3$). Increased RGD tethering did not influence the overall stiffness of the hydrogels. However, 8-arm gels were significantly stiffer compared to the 4-arm gels ($p < 0.05$). Median with 90^{th} and 10^{th} percentiles. C: cyclic RGD, L: linear RGD, NF: non- functionalised.

In addition to assessing the stiffness of hydrogels, the degree of swelling was determined as a measure of gel topology. Soft hydrogels show a significantly larger increase in volume 48 hours after swelling compared to 1.5 h after swelling (Fig. 2). However, 8-arm gels did not swell more at 48 h versus 1.5 h. The data also shows that increased RGD tethering does not result in significant differences in swelling

ratios for both soft and stiff gel groups, which is consistent with the AFM nanoindentation results (Fig. 1). 4-arm (10 kDa) gels display intermediate gel stiffness, with mean swelling ratios higher than those of stiff gels but lower than those of soft gels at both time points.

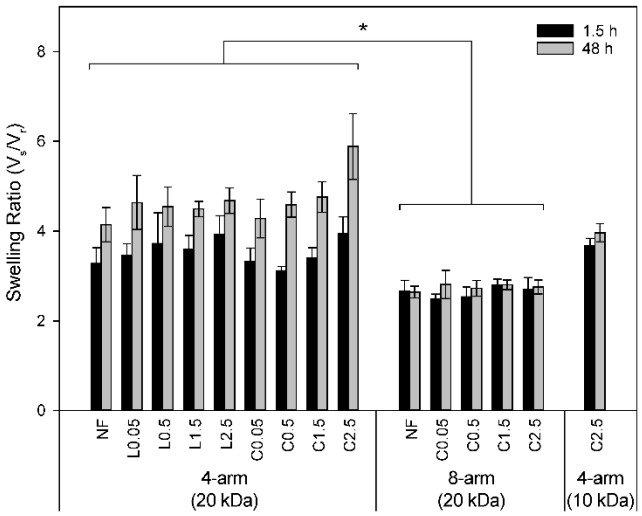

Fig. 2: Average swelling ratios (± SD) of PEG-MAL hydrogels swollen for 1.5 h and 48 h (n=6). Increased RGD tethering does not have a significant effect on swelling for any gel type. Furthermore, after 1.5 h no significant differences in swelling can be observed between stiff and soft gels. Statistically, 4-arm gels exhibit increased swelling at 48 h in comparison to 8-arm counterparts (*$p < 0.05$). 8-arm gels appear to reach maximal swelling at 1.5 h and do not swell further at 48 h. C: cyclic RGD, L: linear RGD, NF: non- functionalised.

3.2 Attachment and spatial organisation of hMSCs

Fig. 3 displays the median number of cells attached to the hydrogels per field of view. On soft RGD-functionalised hydrogels, fewer than 40 cells attached per field of view. Additionally, we observe increased hMSC attachment on soft hydrogels with an increase in RGD concentration. However, there is no significant difference in cell attachment between gels with linear versus cyclic RGDs at each concentration tested. Interestingly, there is a significant increase in cell attachment for stiff hydrogels beyond 0.5 mM of RGD, whereas stiff gels functionalised with RGD concentrations as low as 0.05 mM support cell adhesion in a similar manner as seen for the soft gels. NF gels lack RGD functionality and

show minimal cell attachment overall, irrespective of differences in stiffness between the 4-arm and 8-arm counterparts. Interestingly, 4-arm (10 kDa) gels functionalised with 2.5 mM of cyclic RGD, which feature a stiffness between the soft and stiff gels ($E \approx 15$ kPa), exhibit significantly fewer number of attached cells compared to all 8-arm gels ($p < 0.05$) . Variation between independent experiments have been accounted for and results from individual experiments are shown in Supplementary figure 2.

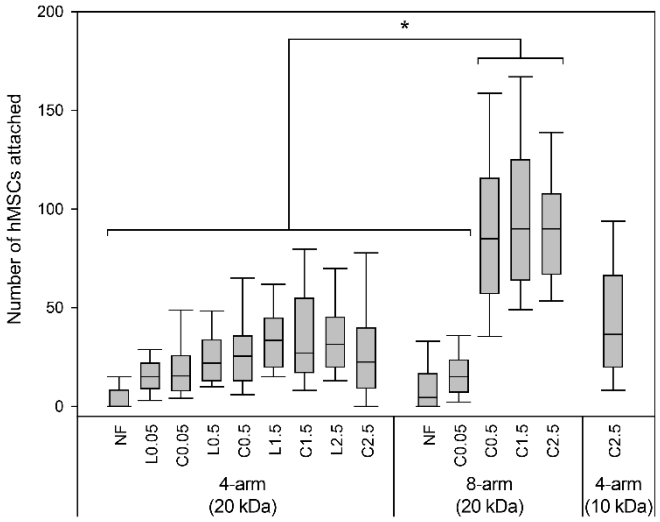

Fig. 3: Number of hMSCs observed per field of view (F.O.V) via confocal microscopy (n=60). A significantly higher cell attachment number was evident for 8-arm gels with RGD concentration of 0.5 mM or more (*$p < 0.05$). Stiff gels with 0.05 mM RGD show cell attachment numbers similar to those observed on soft gels. C: cyclic RGD, L: linear RGD, NF: non- functionalised.

Fig. 4 shows qualitative differences in hMSC organization based on the substrate stiffness and availability of RGD motifs. These images indicate spreading on gels of sufficient stiffness in conjunction with an adequate concentration of RGD motifs (≥ 0.5 mM). On all soft hydrogels, cells cluster and organize themselves in close proximity to each other, irrespective of concentration and type of RGD. Fig. 4 also shows that cells do not spread on 4-arm (10 kDa) gels, despite an ample amount of RGD and a higher stiffness compared to 4-arm (20 kDa) gels. Furthermore, on soft 4-arm gels we generally observe an increased cluster size with increased concentration of RGD for both linear and cyclic RGD.

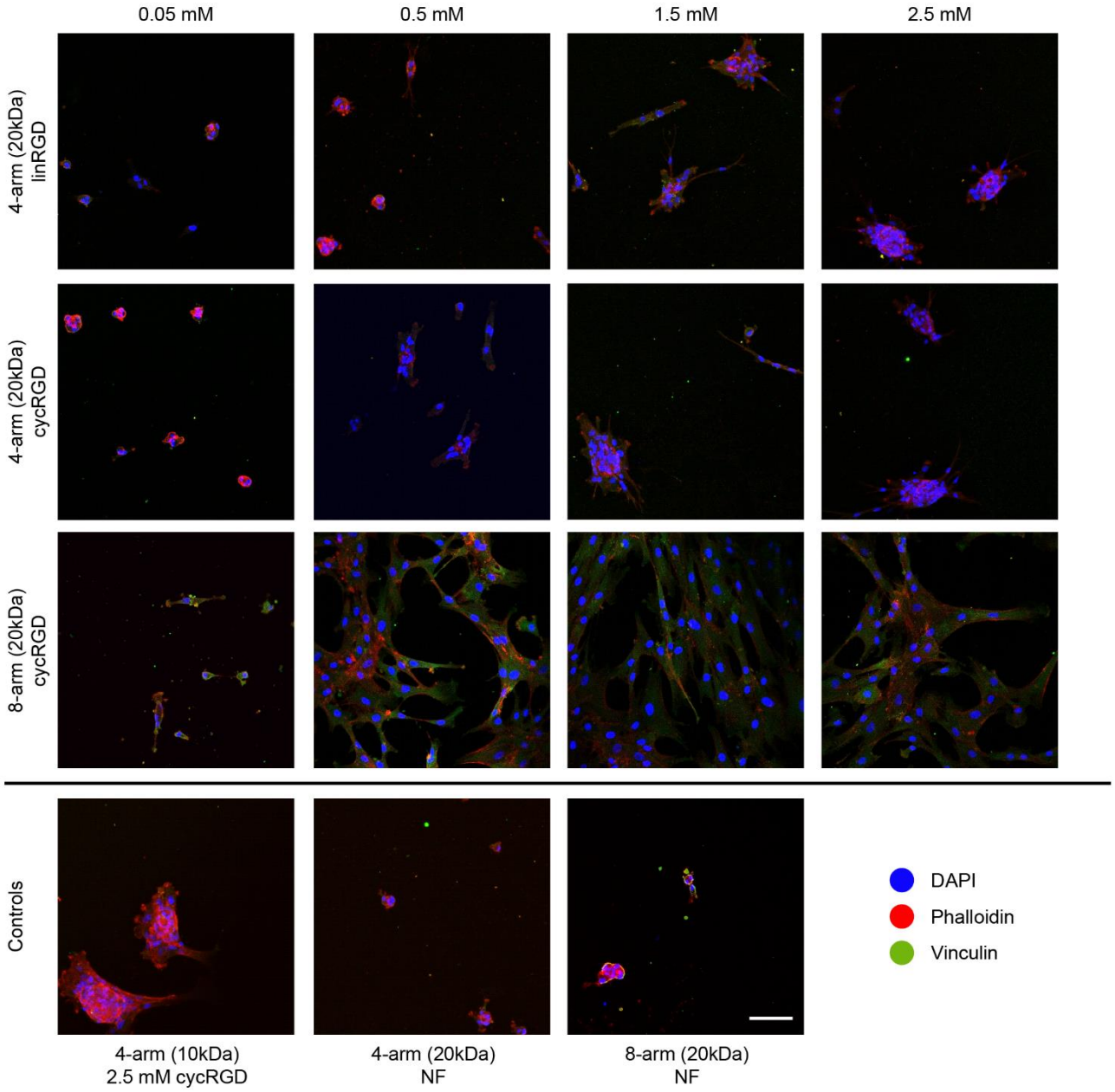

Fig. 4: Confocal images of hMSCs immunolabeled with DAPI (nucleus), phalloidin (actin) and vinculin (focal adhesions) (scale bar: 100 µm). hMSCs organised themselves as clusters on soft substrates, irrespective of RGD conformation or concentration. Furthermore, a shift in hMSC organisation is evident on stiff hydrogels with 0.5 mM of cycRGD or more. cyc: cyclic RGD, lin: linear RGD, NF: non-functionalised.

In order to quantify the manner in which cells organize themselves, we measured the proximity of each cell in relation to the cells around it. This results in an R-value indicative of each hMSC's association with its neighbours (Fig. 5A). When assessing spatial organisation of hMSCs, we see higher R-values for stiff hydrogels. R-values were distinctively high in stiff gels with an RGD concentration of up to 0.5 mM, indicating a more random cell distribution compared to cells seeded on the soft gels, which exhibit lower R-values denoting clustering. Overall, stiff gels feature significantly higher R-values with increased RGD concentrations, indicative of greater spreading ($p < 0.05$). Finally, though few hMSCs attached to NF gels, R-values are less than 0.32, indicating clustering which can also be seen qualitatively in Fig. 4.

An additional parameter assessed is the surface area covered by attached cells. This enables quantifying the extent of spreading while also providing an overview of the degree of clustering on softer hydrogels. hMSCs attached to stiff hydrogels with more than 0.5 mM RGD cover approximately 40% of the surface area of the gel. This is a significantly higher coverage compared to groups where cells cluster (Fig. 5B). Groups that exhibit clustering show minimal coverage on the surface of the gel, implying that clusters are relatively small.

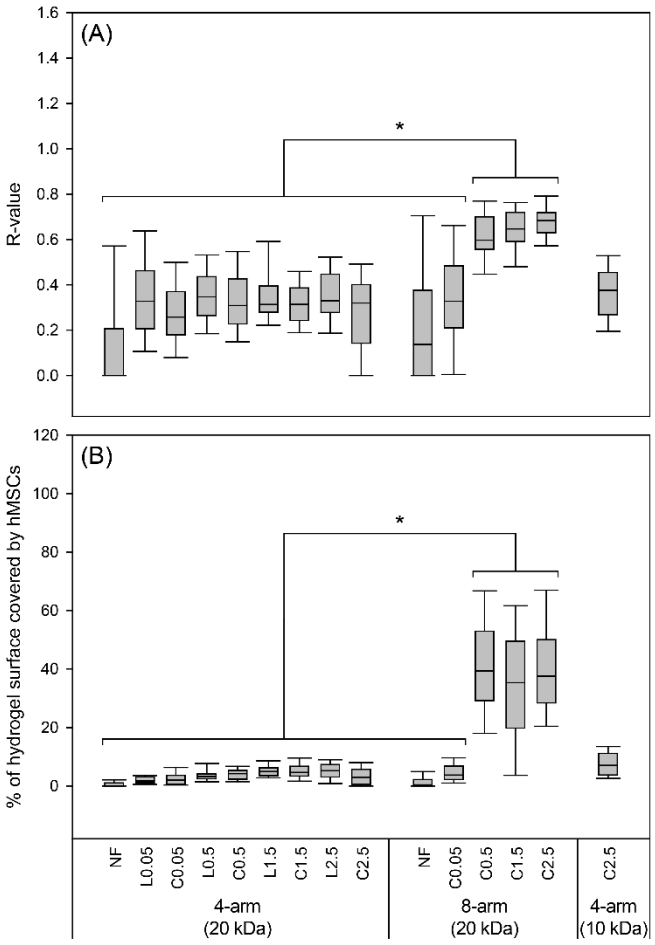

Fig. 5: (A) R-values classifying spatial organisation of hMSCs across the field of view (n = 60). On soft gels, hMSCs exhibit significantly higher clustering irrespective of RGD concentrations with R-values ≤ 0.3 (*p < 0.05). NF gels also exhibit clustering with even lower R-values. Stiff gels exhibit decreased clustering as RGD concentrations increase, with an evident shift in cellular organisation between 0.05 and 0.5 mM. (B) Surface area of the gel covered by hMSCs. Differences in cell organization leads to distinct differences in cell coverage. Cells attached on stiff substrates functionalized with sufficient RGD tend to spread, resulting in higher surface coverage (≈ 40%). However, on soft gels clustered cells cover a smaller surface area (< 8%). C: cyclic RGD, L: linear RGD, NF: non- functionalised.

To further investigate cellular interactions with the PEG hydrogels, cells were immunolabeled with an anti-vinculin primary antibody (Fig. 6). For all gel types, irrespective of stiffness or RGD concentration, no peripheral recruitment of vinculin was observed. Vinculin appears across the cytoplasm with no

indication of mature focal adhesion formation. However, cells seeded on glass cover slips showed distinct peripheral localisation of vinculin as part of mature focal adhesions complexes.

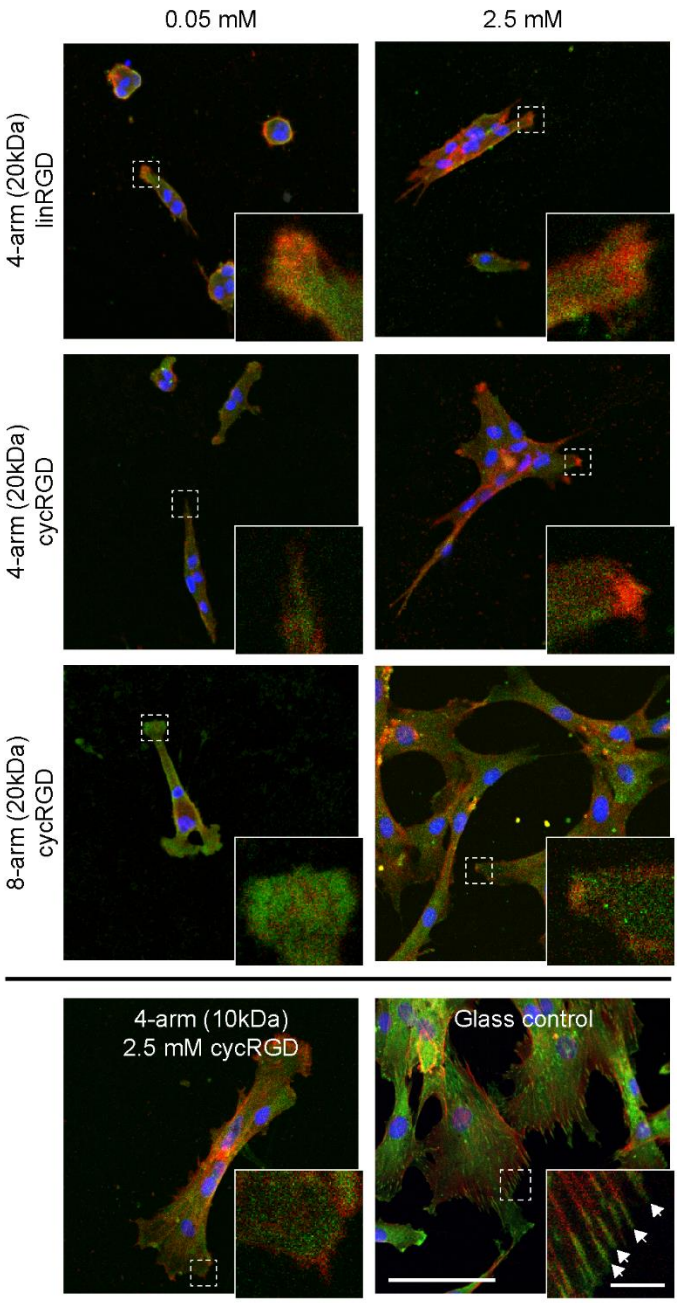

Fig. 6: hMSCs immunolabeled with DAPI (blue), phalloidin (red) anti-vinculin antibodies (green) (scale bar: 100 µm). Inlet images highlight cell peripheries (inlet scale bar: 10 µm). No recruitment of vinculin

was observed as part of mature focal adhesion formation for all gel types. Instead, vinculin was observed across the cytoplasm of cells, without particular localisation at the periphery. Cells seeded on glass coverslips clearly exhibit mature focal adhesion formation with vinculin distinctively localised to complexes at the periphery of the cell body (white arrows). cyc: cyclic RGD, lin: linear RGD.

4. Discussion

Mesenchymal stem cells are an adherent-dependent cell type, implying that physical and biochemical interactions with their microenvironment can influence cell survival, growth, migration and differentiation (Dominici et al., 2006; Park et al., 2012). Salinas and Anseth have previously tested MSC affinity for different RGD peptide sequences and their contextual presentation in PEG hydrogels (Salinas and Anseth, 2008). However, the combined influence of RGD concentration and stiffness on the spatial organisation of hMSCs on hydrogel substrates has not yet been investigated.

We first determined whether increased RGD tethering affects hydrogel stiffness. Since maleimide groups functionalised with RGD peptides are no longer available for end-linking, one might expect a decreased number of elastically effective chains in the network and thus a reduced stiffness. However, we do not see any statistically significant differences within either of the gel groups when varying RGD concentrations. This means that despite the different numbers of maleimide groups available for end-linking, a comparable number of end-links is formed. This observation can be explained by the fact that the architecture of the used hydrogels is non-ideal in the sense that just a fraction of the available functional groups ultimately forms elastically effective links. Thus, the number of ultimately formed end-links can well be very similar, irrespective of a fraction of the maleimide groups being consumed for tethering RGD motifs. However, the large variation of measured stiffness values makes it difficult to draw any definite conclusions. Though we do not see changes in stiffness upon RGD functionalization, it is important to acknowledge the possibilities of alterations in network architecture, such as entanglements and changes in hydrophobicity that may occur. However, analysis of this is beyond the scope of this study. Zustiak and colleagues successfully tested different peptides and studied the effects on a variety of gel parameters (Zustiak et al., 2010). However, no previous studies have investigated the effects of different RGD isoforms on substrate stiffness.

Unsurprisingly, we observed substantial differences in stiffness between the 4-arm and 8-arm gel groups. It is also worth noting the large spread in measured stiffness for each of the groups. This represents a substantial variation when producing the gels independently. However, replicates for any

given gel group produced from the same reaction mix did not exhibit such large variations. In contrast, we see consistent results in cell attachment and organisation for independent batches of the gel. To our best knowledge, there have been two previous studies on changes in substrate compliance with increased ligand tethering for PEG hydrogels (Missirlis and Spatz, 2014; Zustiak et al., 2010). Zustiak and colleagues tested the effects of 0.1, 1.0 and 3.0 mM RGD on the swelling ratios and shear moduli of PEG gels. They found that swelling ratios were increased by 12% only in gels functionalised with 3.0 mM of RGD compared to hydrogels with no RGD, and shear moduli were not altered for concentrations below 3.0 mM (Zustiak et al., 2010). In a different study, Missirlis and Spatz tested gels of similar stiffness as in our study and report that increased RGD concentrations only resulted in a slight increase in E modulus for 'medium' ($E \approx 33.2$ kPa) and 'stiff' ($E \approx 65.4$ kPa) gels (Missirlis and Spatz, 2014). Considering we here incorporate a maximum of 2.5 mM RGD, our results are in good accordance with those reported. Contradictory to observations from Missirilis and Spatz, we report a significant increase in cell attachment with increased substrate stiffness. This effect is enhanced upon increasing RGD concentrations on stiff substrates (Fig. 3). Even though we did not see major effects on substrate stiffness with increased RGD tethering, cells do sense a combination of these factors and exhibit organisational differences.

hMSCs on soft PEG gels cluster rather than spread, irrespective of RGD peptide concentrations or isoforms (Fig. 4). It is likely that a variety of factors contribute to this observation. For instance, cells require sufficient traction to enable spreading which may be inadequate on the soft gels (Fang and Lai, 2016). Additionally, due to significantly greater swelling for soft gels (Fig. 2), RGDs are spaced further apart than those on the stiff gels, despite identical nominal concentrations. Assuming that peptides within 5 nm from the surface are available for cell interaction, we found 30 to 1690 peptides/μm^2 for soft gels and 60 to 2830 peptides/μm^2 for stiff gels based on the nominal RGD concentrations ranging from 0.05 to 2.5 mM. Previous studies controlled RGD presentation and found that cell spreading is highly sensitive to slight changes in ligand spacing (Arnold et al., 2004; Wilson et al., 2012; Wolfenson et al., 2014). They identified a critical spacing of 60 to 70 nm to be required for stable integrin mediated adhesion. Elsewhere, Frith et al. studied the influence of lateral spacing of RGD on hMSCs and found that cells were less spread for ligand spacing greater than 62 nm (Frith et al., 2012). Based on a theoretical estimate, soft hydrogels used in our study with RGD concentrations of 0.5 mM or higher are below this threshold, indicating that RGD concentration alone does not govern the cell morphology.

Missirlis and Spatz observed similar rounded cell morphologies when seeding REF52 cells on hydrogels functionalized with up to 0.5 mM RGD (Missirlis and Spatz, 2014). However, in contrast to our findings, these cells were not clustered. Two primary reasons may contribute to the cluster morphologies of hMSCs on soft gels. First, the lack of traction prevents the cells from spreading and thus limiting the movement of cells on the surface. Second, the lack of sufficient available anchoring points may cause the cells to cluster. As a result, cells in close proximity with each other appear to attach to their neighbours in order to survive and form clusters. For stiffer gels providing sufficient traction, 0.05 mM RGD is inadequate to prevent clustering. However, stiff gels with RGD concentrations of 0.5 mM or higher support hMSC spreading. As a result, a combination of sufficient stiffness to provide traction and adequate RGD motifs seems to be required to enable cell adhesion and prevent clustering.

Although the presence or absence of ligands plays an independent role, previous studies have shown that cell shape and spreading are greatly regulated by substrate stiffness (Han et al., 2012). Engler et al. demonstrated that cells on soft substrates are insensitive to adhesion ligand density (Engler et al., 2004). We observed a similar scenario here, where the presence of RGD alone does not enable cells to spread if the substrate is not sufficiently stiff. The cytoskeleton plays a central role in cell spreading, and as a response to mechanical stimuli, proteins assemble at the periphery of the cytoskeleton to form focal complexes (Engler et al., 2004). Confocal images taken of hMSCs seeded on soft gels in Fig. 6 showed no punctuations of large, mature focal adhesions akin to those observed on glass controls. Instead, we observe dot-like expression of vinculin throughout the cell body of cells seeded on hydrogels. Intriguingly, Fig. 6 also shows hMSCs spread on stiff hydrogels, but there is no indication of vinculin at the cell membrane to represent mature focal adhesions. One possible reason leading to the absence of mature focal adhesions may be attributed to the lack of mechanical forces to drive the recruitment of vinculin associated with mechanosensing at focal complexes. Other studies also suggest vinculin recruitment to focal adhesions in cells on substrates with Youngs moduli of at least 200 kPa (Kocgozlu et al., 2010). This would explain the lack of mature focal adhesions on soft hydrogels. However, hMSCs did not form mature focal adhesions on stiff hydrogels either. This is likely due to the insufficient binding of integrin to the substrate, since vinculin is known to play a vital role in physically linking integrins to the cytoskeleton (Berrier and Yamada, 2007).

Cavalcanti-Adam and colleagues have previously observed a lack of focal adhesions on substrates with RGD spaced 108 nm or further apart. However, integrin-based adhesion may still occur at this point, leading to what has been referred to as cryptic adhesions forming under protruding lamellae (Cavalcanti-Adam et al., 2007). In the study conducted by Missirlis and Spatz, REF52 cells were seeded on to PEG hydrogels functionalised with 0.1 to 2.0 mM RGD (Missirlis and Spatz, 2014). They observed localisation of vinculin to the periphery on gels with RGD concentrations of at least 0.25 mM. However, we observed neither focal adhesion formation nor vinculin recruitment at the cell periphery, irrespective of RGD presentation. The PEG gels used in their study feature a similar stiffness as the soft and stiff gels tested in our study. However, since the cells they used are of rat origin, there may be interspecies differences to consider in the regulation of vinculin when compared to hMSCs. However, we observed vinculin throughout the cytoplasm. One possible explanation is that we are observing nascent focal adhesions, since evidence suggest that they occur independent of substrate rigidity (Changede et al., 2015). However, definite verification of nascent focal adhesions is complicated and previous studies suggested localisation at the lamellipodium (Choi et al., 2008). The lack of mature focal adhesions has further been attributed to increased cell motility (Rodriguez Fernandez et al., 1992), contributing to the observed formation of cell clusters.

Previous studies typically encapsulate cells into PEG hydrogels in order to study how cells interact with their 3D environment (Pfaff et al., 1994; Wang et al., 2013; Yang et al., 2005). However, few studies have seeded cells onto the surface of hydrogels (Huebsch et al., 2010). In clinical situations, access and isolation of patient's stem cells can be expensive and limited. As a result, it is important to recognize alternative approaches that are capable of inducing local host stem cell migration towards the site of damage using injectable, cell-responsive, biodegradable scaffolds. There has been increasing evidence that mesenchymal stem cells have immense migratory potential in various regenerative scenarios, both *in vitro* and *in vivo* (Cornelissen et al., 2015). In order to orchestrate the function of MSCs, it is necessary to understand how these cells attach, colonise and organise themselves on compliant materials. Therefore, the minimum requirements for efficient adhesion and the optimal mechanical stiffness need to be determined. Our study, however, shows that these processes are multifaceted and do not solely depend on substrate stiffness or RGD presentation independently. This fundamental understanding constitutes a prerequisite for a future class of acellular scaffolds.

5. Conclusions

This study extends the current knowledge for cell-based applications that utilize PEG. We provide a basis for selecting specific stiffness and ligand presentation that contribute to hMSCs attachment and colonisation on PEG hydrogels. In order to attach large numbers of hMSCs in a spread manner, both substrate stiffness and attachment ligand concentrations need to be above a certain threshold. Cells seeded on soft hydrogels exhibited significantly fewer attached cells, with the formation of cell clusters, irrespective of RGD concentrations. In contrast, hMSCs attached in large numbers and spread on stiff hydrogels with RGD concentrations of 0.5 mM or higher, suggesting that cell attachment and spreading are both multifaceted phenomena. We observed that increased RGD tethering has no significant effect on the stiffness of both soft and stiff hydrogels. Additionally, we found no differences in the number of hMSCs attaching to gels functionalised with either linear or cyclic RGD.

6. Acknowledgements

The authors are grateful to Dr. Nick J. Walters for the constructive discussions and his critical review of this manuscript. This research did not receive any specific grant from funding agencies in the public, commercial, or not-for-profit sectors.

References:

Anderson, S.B., Lin, C.C., Kuntzler, D.V., Anseth, K.S., 2011. The performance of human mesenchymal stem cells encapsulated in cell-degradable polymer-peptide hydrogels. Biomaterials 32, 3564-3574.

Arnold, M., Cavalcanti-Adam, E.A., Glass, R., Blümmel, J., Eck, W., Kantlehner, M., Kessler, H., Spatz, J.P., 2004. Activation of integrin function by nanopatterned adhesive interfaces. ChemPhysChem 5, 383-388.

Bae, M.-S., Lee, K.Y., Park, Y.J., Mooney, D.J., 2007. RGD Island Spacing Controls Phenotype of Primary Human Fibroblasts Adhered to Ligand-Organized Hydrogels. Macromolecular Research 15, 469-472.

Bellis, S.L., 2011. Advantages of RGD peptides for directing cell association with biomaterials. Biomaterials 32, 4205-4210.

Berrier, A.L., Yamada, K.M., 2007. Cell–matrix adhesion. J. Cell Physiol. 213, 565-573.

Cavalcanti-Adam, E.A., Volberg, T., Micoulet, A., Kessler, H., Geiger, B., Spatz, J.P., 2007. Cell spreading and focal adhesion dynamics are regulated by spacing of integrin ligands. Biophys. J. 92, 2964-2974.

Changede, R., Xu, X., Margadant, F., Sheetz, Michael P., 2015. Nascent Integrin Adhesions Form on All Matrix Rigidities after Integrin Activation. Dev. Cell 35, 614-621.

Chicurel, M.E., Chen, C.S., Ingber, D.E., 1998. Cellular control lies in the balance of forces. Curr. Opin. Cell Biol. 10, 232-239.

Choi, C.K., Vicente-Manzanares, M., Zareno, J., Whitmore, L.A., Mogilner, A., Horwitz, A.R., 2008. Actin and α-actinin orchestrate the assembly and maturation of nascent adhesions in a myosin II motor-independent manner. Nat. Cell Biol. 10, 1039.

Clark, P.J., Evans, F.C., 1954. Distance to Nearest Neighbor as a Measure of Spatial Relationships in Populations. Ecology 35, 445-453.

Cornelissen, A.S., Maijenburg, M.W., Nolte, M.A., Voermans, C., 2015. Organ-specific migration of mesenchymal stromal cells: Who, when, where and why? Immunol. Lett. 168, 159-169.

Deeg, J.A., Louban, I., Aydin, D., Selhuber-Unkel, C., Kessler, H., Spatz, J.P., 2011. Impact of local versus global ligand density on cellular adhesion. Nano Lett. 11, 1469-1476.

Dominici, M., Le Blanc, K., Mueller, I., Slaper-Cortenbach, I., Marini, F., Krause, D., Deans, R., Keating, A., Prockop, D., Horwitz, E., 2006. Minimal criteria for defining multipotent mesenchymal stromal cells. The International Society for Cellular Therapy position statement. Cytotherapy 8, 315-317.

Eidet, J.R., Pasovic, L., Maria, R., Jackson, C.J., Utheim, T.P., 2014. Objective assessment of changes in nuclear morphology and cell distribution following induction of apoptosis. Diagn. Pathol. 9, 92-92.

El-Sherbiny, I.M., Yacoub, M.H., 2013. Hydrogel scaffolds for tissue engineering: Progress and challenges. Glob. Cardiol. Sci. Pract. 2013, 316-342.

Engler, A., Bacakova, L., Newman, C., Hategan, A., Griffin, M., Discher, D., 2004. Substrate compliance versus ligand density in cell on gel responses. Biophys. J. 86, 617-628.

Engler, A.J., Sen, S., Sweeney, H.L., Discher, D.E., 2006. Matrix elasticity directs stem cell lineage specification. Cell 126, 677-689.

Fang, Y., Lai, K.W.C., 2016. Modeling the mechanics of cells in the cell-spreading process driven by traction forces. Phys. Rev. E 93, 042404.

Frith, J.E., Mills, R.J., Cooper-White, J.J., 2012. Lateral spacing of adhesion peptides influences human mesenchymal stem cell behaviour. J. Cell Sci. 125, 317-327.

Fusco, S., Panzetta, V., Embrione, V., Netti, P.A., 2015. Crosstalk between focal adhesions and material mechanical properties governs cell mechanics and functions. Acta Biomater. 23, 63-71.

Han, Sangyoon J., Bielawski, Kevin S., Ting, Lucas H., Rodriguez, Marita L., Sniadecki, Nathan J., 2012. Decoupling substrate stiffness, spread area, and micropost density: A close spatial relationship between traction forces and focal adhesions. Biophys. J. 103, 640-648.

Haubner, R., Gratias, R., Diefenbach, B., Goodman, S.L., Jonczyk, A., Kessler, H., 1996. Structural and functional aspects of RGD-containing cyclic pentapeptides as highly potent and selective integrin $\alpha_V\beta_3$ antagonists. J. Am. Chem. Soc. 118, 7461-7472.

Hern, D.L., Hubbell, J.A., 1998. Incorporation of adhesion peptides into nonadhesive hydrogels useful for tissue resurfacing. J. Biomed. Mater. Res. 39, 266-276.

Herrick, W.G., Nguyen, T.V., Sleiman, M., McRae, S., Emrick, T.S., Peyton, S.R., 2013. PEG-phosphorylcholine hydrogels as tunable and versatile platforms for mechanobiology. Biomacromolecules 14, 2294-2304.

Hersel, U., Dahmen, C., Kessler, H., 2003. RGD modified polymers: biomaterials for stimulated cell adhesion and beyond. Biomaterials 24, 4385-4415.

Hsiong, S.X., Carampin, P., Kong, H.J., Lee, K.Y., Mooney, D.J., 2008. Differentiation stage alters matrix control of stem cells. J. Biomed. Mater. Res. A 85, 145-156.

Huebsch, N., Arany, P.R., Mao, A.S., Shvartsman, D., Ali, O.A., Bencherif, S.A., Rivera-Feliciano, J., Mooney, D.J., 2010. Harnessing traction-mediated manipulation of the cell/matrix interface to control stem-cell fate. Nat. Mater. 9, 518-526.

Kantlehner, M., Schaffner, P., Finsinger, D., Meyer, J., Jonczyk, A., Diefenbach, B., Nies, B., Holzemann, G., Goodman, S.L., Kessler, H., 2000. Surface coating with cyclic RGD peptides stimulates osteoblast adhesion and proliferation as well as bone formation. Chembiochem 1, 107-114.

Kilian, K.A., Mrksich, M., 2012. Directing stem cell fate by controlling the affinity and density of ligand–receptor interactions at the biomaterials interface. Angew. Chem. Int. Ed. 51, 4891-4895.

Kim, D.-H., Provenzano, P.P., Smith, C.L., Levchenko, A., 2012. Matrix nanotopography as a regulator of cell function. J. Cell Biol. 197, 351.

Kocgozlu, L., Lavalle, P., Koenig, G., Senger, B., Haikel, Y., Schaaf, P., Voegel, J.-C., Tenenbaum, H., Vautier, D., 2010. Selective and uncoupled role of substrate elasticity in the regulation of replication and transcription in epithelial cells. J. Cell Sci. 123, 29-39.

Kyburz, K.A., Anseth, K.S., 2013. Three-dimensional hMSC motility within peptide-functionalized PEG-based hydrogels of varying adhesivity and crosslinking density. Acta Biomater. 9, 6381-6392.

Li, L., Eyckmans, J., Chen, C.S., 2017. Designer biomaterials for mechanobiology. Nat. Mater. 16, 1164.

Mathieu, P.S., Loboa, E.G., 2012. Cytoskeletal and focal adhesion influences on mesenchymal stem cell shape, mechanical properties, and differentiation down osteogenic, adipogenic, and chondrogenic pathways. Tissue Eng. B 18, 436-444.

Missirlis, D., Spatz, J.P., 2014. Combined effects of PEG hydrogel elasticity and cell-adhesive coating on fibroblast adhesion and persistent migration. Biomacromolecules 15, 195-205.

Nuttelman, C.R., Tripodi, M.C., Anseth, K.S., 2004. In vitro osteogenic differentiation of human mesenchymal stem cells photoencapsulated in PEG hydrogels. J. Biomed. Mater. Res. A 68, 773-782.

Park, J., Kim, P., Helen, W., Engler, A.J., Levchenko, A., Kim, D.-H., 2012. Control of stem cell fate and function by engineering physical microenvironments. Integr. Biol. 4, 1008-1018.

Pfaff, M., Tangemann, K., Muller, B., Gurrath, M., Muller, G., Kessler, H., Timpl, R., Engel, J., 1994. Selective recognition of cyclic RGD peptides of NMR defined conformation by alpha IIb beta 3, alpha V beta 3, and alpha 5 beta 1 integrins. J. Biol. Chem. 269, 20233-20238.

Rodda, A.E., Meagher, L., Nisbet, D.R., Forsythe, J.S., 2014. Specific control of cell–material interactions: Targeting cell receptors using ligand-functionalized polymer substrates. Prog. Polym. Sci. 39, 1312-1347.

Rodriguez Fernandez, J.L., Geiger, B., Salomon, D., Sabanay, I., Zoller, M., Ben-Ze'ev, A., 1992. Suppression of tumorigenicity in transformed cells after transfection with vinculin cDNA. J. Cell Biol. 119, 427-438.

Salinas, C.N., Anseth, K.S., 2008. The influence of the RGD peptide motif and its contextual presentation in PEG gels on human mesenchymal stem cell viability. J. Tissue Eng. Regen. Med. 2, 296.

Schwarz, U.S., Bischofs, I.B., 2005. Physical determinants of cell organization in soft media. Med. Eng. Phys. 27, 763-772.

Shu, X.Z., Ghosh, K., Liu, Y., Palumbo, F.S., Luo, Y., Clark, R.A., Prestwich, G.D., 2004. Attachment and spreading of fibroblasts on an RGD peptide-modified injectable hyaluronan hydrogel. J. Biomed. Mater. Res. A 68, 365-375.

Verrier, S., Pallu, S., Bareille, R., Jonczyk, A., Meyer, J., Dard, M., Amédée, J., 2002. Function of linear and cyclic RGD-containing peptides in osteoprogenitor cells adhesion process. Biomaterials 23, 585-596.

Wang, X., Yan, C., Ye, K., He, Y., Li, Z., Ding, J., 2013. Effect of RGD nanospacing on differentiation of stem cells. Biomaterials 34, 2865-2874.

Wen, J.H., Vincent, L.G., Fuhrmann, A., Choi, Y.S., Hribar, K.C., Taylor-Weiner, H., Chen, S., Engler, A.J., 2014. Interplay of matrix stiffness and protein tethering in stem cell differentiation. Nat. Mater. 13, 979-987.

Wilson, M.J., Liliensiek, S.J., Murphy, C.J., Murphy, W.L., Nealey, P.F., 2012. Hydrogels with well-defined peptide-hydrogel spacing and concentration: impact on epithelial cell behavior(). Soft Matter 8, 390-398.

Wolfenson, H., Iskratsch, T., Sheetz, Michael P., 2014. Early events in cell spreading as a model for quantitative analysis of biomechanical events. Biophys. J. 107, 2508-2514.

Yang, F., Williams, C.G., Wang, D.A., Lee, H., Manson, P.N., Elisseeff, J., 2005. The effect of incorporating RGD adhesive peptide in polyethylene glycol diacrylate hydrogel on osteogenesis of bone marrow stromal cells. Biomaterials 26, 5991-5998.

Yim, E.K.F., Darling, E.M., Kulangara, K., Guilak, F., Leong, K.W., 2010. Nanotopography-induced changes in focal adhesions, cytoskeletal organization, and mechanical properties of human mesenchymal stem cells. Biomaterials 31, 1299.

Zhang, D., Sun, M.B., Lee, J., Abdeen, A.A., Kilian, K.A., 2016. Cell shape and the presentation of adhesion ligands guide smooth muscle myogenesis. J. Biomed. Mater. Res. A 104, 1212-1220.

Zustiak, S.P., Durbal, R., Leach, J.B., 2010. Influence of cell-adhesive peptide ligands on poly(ethylene glycol) hydrogel physical, mechanical and transport properties. Acta Biomater. 6, 3404-3414.